

From demagnetizing to magnetizing interactions in CoFe–AgCu granular films

V. Franco, X. Batlle, and A. Labarta

Department Física Fonamental, Universitat de Barcelona, Diagonal 647, 08028 Barcelona, Catalonia, Spain

M. L. Watson

Centre for Data Storage Materials, Coventry University, Priory Street, Coventry CV1 5FB, United Kingdom

K. O'Grady

School of Electronic Engineering Science, University of Wales, Bangor, Gwynedd LL57 1UT, United Kingdom

CoFe–AgCu granular films of compositions ranging from 0.17–0.44 ferromagnetic atomic concentration were prepared by rf sputtering. The microstructure and the transport and magnetic properties suggested that this family of samples can be classified into two groups with a crossover concentration at about 32 at.%. The experimental results for samples $\text{Co}_{34}\text{Fe}_8\text{Ag}_{54}\text{Cu}_4$ and $\text{Co}_{18}\text{Fe}_8\text{Ag}_{70}\text{Cu}_4$, which are representative of both different behaviors, are discussed. For the as-prepared sample with higher CoFe content, an uncompensated out-of-plane antiferromagneticlike microstructure with dominant demagnetizing interactions was observed. The particle growth through the annealing led to large in-plane ferromagneticlike clusters with dominant magnetizing interactions. The thermal dependence of the remanence-to-saturation ratio of the as-prepared and annealed samples indicated the existence of a high degree of magnetic correlations leading to a very low magnetoresistivity: In none of the cases was a Stoner–Wohlfarth behavior observed. On the contrary, for the sample with lower CoFe content, the magnetoresistivity change was much higher, and the remanence followed the expected behavior, since magnetic correlations were strongly reduced through dilution. © 1997 American Institute of Physics. [S0021-8979(97)69608-5]

In the past few years, giant magnetoresistivity (GMR) has been found in granular alloys consisting of a distribution of small ferromagnetic (FM) particles which have been randomly segregated in a nonmagnetic metallic matrix.¹ Examples of granular alloys exhibiting GMR are:² $\text{Co}_x\text{Cu}_{1-x}$, $\text{Co}_x\text{Ag}_{1-x}$, $\text{Fe}_x\text{Ag}_{1-x}$, and $(\text{NiFe})_x\text{Ag}_{1-x}$. In this paper we present a study of the structural, magnetic and GMR properties of CoFe–AgCu granular alloys. We have included Fe as a minor ferromagnetic component in the largely studied Co–Ag system in order to increase GMR as previously reported,³ and a small amount of Cu to increase immiscibility between CoFe and the nonmagnetic matrix. We have recently shown⁴ the existence of an uncompensated antiferromagneticlike microstructure at volume concentrations below the percolation threshold [$x_p=0.55$ (Ref. 5)] in the granular system $\text{Co}_{34}\text{Fe}_8\text{Ag}_{54}\text{Cu}_4$ ($x=0.33$), and we have reported on magnetic interactions arising from the microstructure affecting GMR and magnetic properties. The aim of this work is to discuss that the stabilization of that magnetic microstructure is related to the ferromagnetic content and thus to the magnetic correlations.

Eleven CoFe–AgCu films of compositions ranging from 0.17–0.44 ferromagnetic atomic concentration were rf sputtered onto glass microscope slides. Post-deposition phase segregation was promoted by rapidly annealing (0.1 s) at 600, 650, and 750 °C. A detailed explanation on the experimental procedure is given in Ref. 6. The particle size distribution and the microstructure of the films were studied by x-ray diffraction (XRD), transmission electron microscopy (TEM), and atomic force microscopy (AFM). Images of the magnetic flux density perpendicular to the film plane were

obtained by magnetic force microscopy (MFM), at room temperature. Magnetoresistivity (MR) was measured using an ac four-probe technique with the magnetic field applied in the film plane along the current direction. The magnetization curves were measured by a vibrating sample magnetometer (VSM) with the magnetic field parallel to the film plane.

Taking into account the microstructure, GMR, and the magnetic properties, this family of samples can be classified into two groups with a crossover concentration at about 32 at.%. We present in this work the experimental results for samples $\text{Co}_{34}\text{Fe}_8\text{Ag}_{54}\text{Cu}_4$ (sample A) and $\text{Co}_{18}\text{Fe}_8\text{Ag}_{70}\text{Cu}_4$ (sample B), which are representative of both different behaviors. TEM micrographs evidence the granular nature of all samples. The AFM images for the as prepared samples A and B show the existence of a random distribution of ferromagnetic (FM) particles which have been segregated from the matrix (Fig. 1). XRD data and TEM indicate that the mean diameter is about 3 nm in both as prepared samples. A rough estimation of the mean distances between particles may be obtained from the volume concentration, leading to 3.4 and 4.2 nm for samples A and B, respectively, in agreement with TEM. The annealing procedure strongly changes the microstructure: The particles surrounded by other particles grow, leading to a broad distribution of irregular large aggregates and a certain amount of small particles, as observed in the AFM images. These aggregates are larger than about 100 nm in sample A annealed at 750 °C and XRD data indicate that the mean diameter of the particles forming them is about 15 nm. However, the mean diameter is about 10 nm

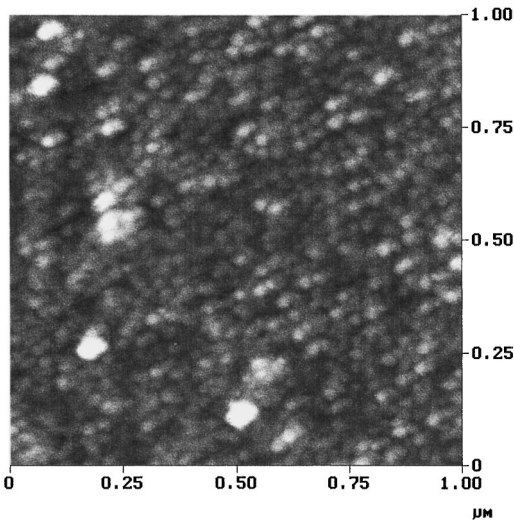


FIG. 1. AFM micrograph at room temperature for the as-prepared sample A.

for sample B annealed at 750 °C due to the fact that the mean particle distance is longer and the FM content is lower than in sample A.

MFM image for the as prepared sample A (Fig. 2) reveals the existence of a magnetic microstructure perpendicular to the film plane.⁴ The magnetic moment of the particles tend to be arranged parallel along an out-of-plane direction forming elongated clusters which are themselves aligned antiparallel with respect to the nearest neighboring clusters (see alternated bright–dark regions in Fig. 2). As a consequence of this magnetic microstructure, the flux density lines tend to be closed through neighboring clusters of antiparallel moments, leading to dominant demagnetizing interactions. The MFM image for sample A annealed at 750 °C does not show any additional contrast with respect to the AFM image, indicating that the out-of-plane component of the particle moments is lost. The large aggregates shown in the AFM image may form large ferromagnetic clusters with the magnetic moment lying in the film plane in order to minimize magne-

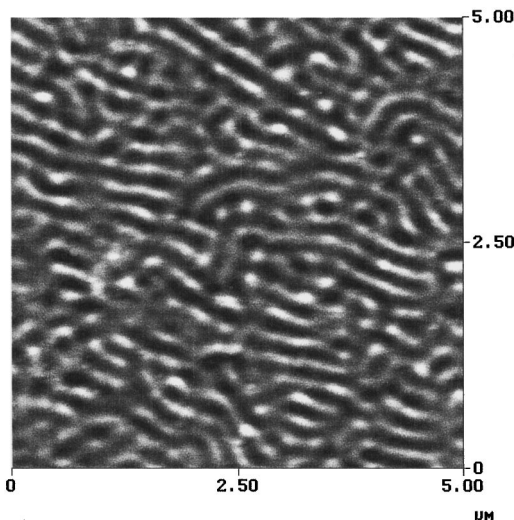


FIG. 2. MFM micrograph at room temperature for the as-prepared sample A. Bright–dark regions indicate opposite magnetic pole orientation.

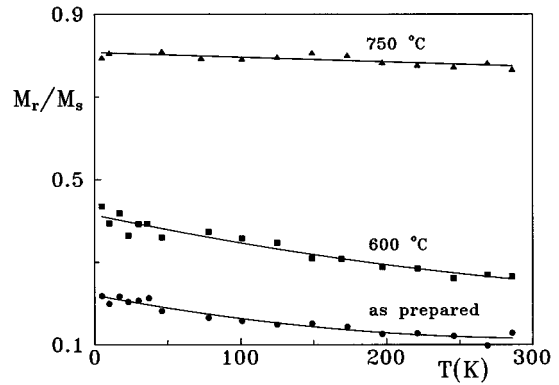


FIG. 3. Thermal dependence of the RTS ratio for the sample A (as-prepared and annealed at 600 and 750 °C). Solid lines are guides for the eye.

tostatic energy. This magnetic arrangement should lead to dominant magnetizing interactions. The micromagnetic structure of sample A suggested by MFM images is also confirmed by the change in sign of the overall interactions through annealing, deduced from the Henkel plots (ΔM plots),⁷ and also explains the field dependence of both the magnetization and the magnetoresistivity (MR). A detailed discussion on these topics may be found in Ref. 4.

We focus here on the study of the remanent-to-saturation (RTS) magnetization ratio. We show in Fig. 3 the temperature variation of the RTS ratio obtained from the hysteresis loops for the as-prepared and two annealing temperatures of sample A. In all three curves a very slight thermal dependence is displayed, which suggests that the strength of the magnetic interactions is high enough to overcome the remanence decay due to thermal activation. For the as-prepared sample A, the value of the RTS ratio extrapolated at $T=0$ is about 0.22, which is much lower than the 0.5 value predicted in the Stoner–Wohlfarth (SW) model for an assembly of noninteracting single-domain particles with uniaxial anisotropy. This reduction in the RTS ratio may be understood taking into account that the remanent magnetization of the as-prepared sample A is related to the existence of metastable states of the quasiantiferromagnetic arrangement of elongated clusters rather than to individual particles. On the

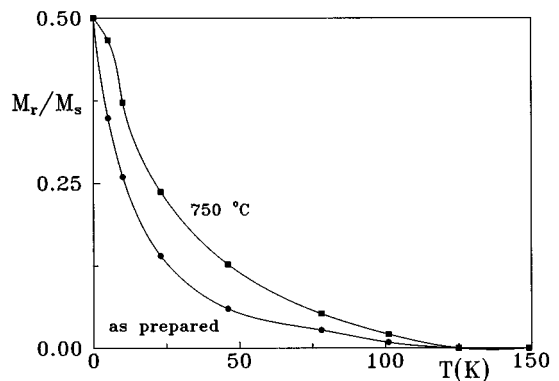


FIG. 4. The same as Fig. 3 for sample B (as-prepared and annealed at 750 °C). The point $T=0$, $M_r/M_s=0.5$ was included in both curves to test the applicability of the SW.

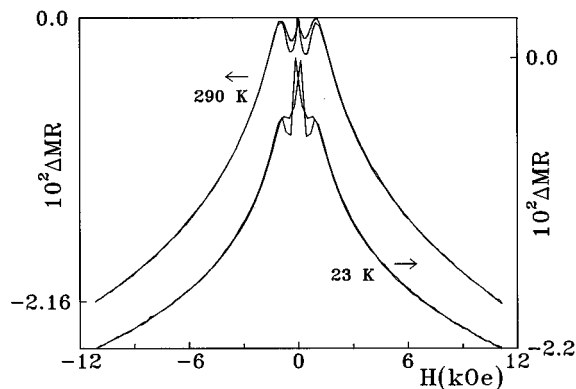


FIG. 5. The relative MR change $\Delta MR = [MR(H) - MR_{\max}] / MR_{\max}$ as a function of the applied field for the as-prepared sample A, at 23 and 290 K.

contrary, the RTS ratio for the annealed sample A at 750 °C is much higher than 0.5 and the extrapolated value at $T=0$ is about 0.8 (the hysteresis loops have a high degree of squareness).⁴ This enhancement of the RTS ratio agrees with the magnetic microstructure shown in the MFM-AFM images: The formation of large aggregates allows direct ferromagnetic exchange through the surface of neighboring particles of the same aggregate, leading to a magnetic microstructure consisting of large FM clusters with the net magnetic moment randomly oriented along in-plane directions. In this situation, the granular alloy mostly behaves as a bulk ferromagnet. This exchange enhancement of the RTS ratio has been also observed in a variety of nanostructured materials.⁸ For sample A annealed at 600 °C an intermediate behavior is depicted and the RTS value extrapolated to $T=0$ is about 0.41: The aggregation process partially destroys the antiparallel arrangement of elongated clusters.

A completely different situation is observed for sample B. Although the mean size of the particles in the as prepared sample is about the same than that of sample A and the particles grow through annealing, the RTS ratios for the as-prepared sample B and the one annealed at 750 °C (see Fig. 4) show the typical SW behavior. This behavior of the diluted sample suggests that the anomalies observed for sample A⁴ are due to dipolar and ferromagnetic exchange interactions among particles, which are probably more important than in sample B due to shorter particle distances and higher FM content.

The magnetic microstructure of sample A leads to *anomalous* GMR and magnetic properties.⁴ The shape of the MR curves at low fields for the as-prepared sample strongly depends on the magnetic history and shows a bimodal structure which is due to the magnetization processes associated with both the antiparallel arrangement of elongated clusters and the uncompensated and isolated moments. An example of the MR curves obtained at 23 and 290 K are shown in Fig. 5. The small values of the MR change (-2.2% at 23 K and -2.16% at 290 K) and the slight thermal dependence are a consequence of the high degree of magnetic correlations

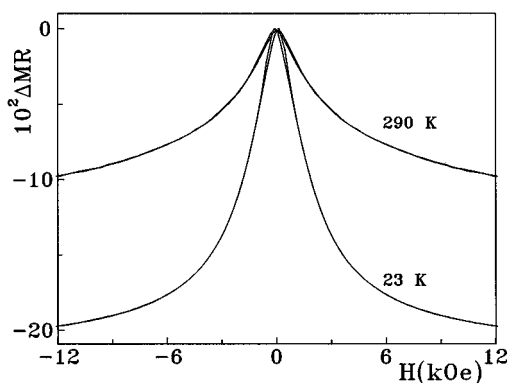


FIG. 6. The same as Fig. 5 for the as-prepared sample B.

present in the system even at room temperature, as the MFM image and RTS ratio suggest: Only the uncorrelated moments give a net contribution to MR. On the contrary, the MR changes for the as-prepared sample B at 23 and 290 K (see Fig. 6) are much higher than those corresponding to sample A and a large variation between both temperatures is also observed (-19.8% at 23 K and -9.8% at 290 K). Although the size of the magnetic particles is similar in both as-prepared samples A and B, the higher dilution of the latter and the longer distance between the particles, lead to a decrease in the magnetic correlations among them. Therefore, in sample B, a larger amount of CoFe particles contributes to MR, increasing the MR change with respect to sample A. Moreover, the bimodal structure of the MR curves at low fields is not present in sample B since magnetic interactions are not high enough to stabilize the elongated cluster structure. The rest of the studied compositions suggest that the anomalous behavior observed in $\text{Co}_{34}\text{Fe}_8\text{Ag}_{54}\text{Cu}_4$ is an intrinsic property of these CoFe-AgCu granular alloys, which is associated with the magnetic correlations, and it appears about above 32 at. % of FM content. A detailed study for a variety of compositions will be published elsewhere soon.

This work was supported by Spanish CICYT through the MAT94-1024-CO2-02 and the Catalan CIRIT through the GRQ1012 projects.

- ¹A. E. Berkowitz, J. R. Mitchell, M. J. Carey, A. P. Young, S. Zhang, F. E. Spada, F. T. Parker, H. Hutten, and G. Thomas, *Phys. Rev. Lett.* **68**, 3745 (1992); J. Q. Xiao, J. S. Jiang, and C. L. Chien, *ibid.* **68**, 3749 (1992).
- ²M. J. Carey, A. P. Young, A. Starr, D. Rao, and A. E. Berkowitz, *Appl. Phys. Lett.* **61**, 2935 (1992); A. Tsoukatos, H. Wan, G. C. Hadjipanayis, K. M. Unruh, and Z. G. Li, *J. Appl. Phys.* **73**, 5509 (1993); J. S. Jiang, J. Q. Xiao, and C. L. Chien, *Appl. Phys. Lett.* **61**, 2362 (1992); M. Kitada, K. Yamamoto, and N. Shimizu, *J. Magn. Magn. Mater.* **124**, 243 (1993).
- ³S. R. Teixeira, B. Dieny, A. Chamberod, C. Cowache, S. Auffret, P. Auric, J. L. Rouviere, O. Redon, and J. Pierre, *J. Phys., Condens. Matter.* **6**, 5545 (1994).
- ⁴X. Batlle, V. Franco, A. Labarta, M. L. Watson, and K. O'Grady, *Appl. Phys. Lett.* **70**, 132 (1997).
- ⁵C. L. Chien, *J. Appl. Phys.* **69**, 5267 (1991).
- ⁶M. L. Watson, K. O'Grady, and V. G. Lewis, *J. Appl. Phys.* **75**, 6927 (1994).
- ⁷M. El-Hilo, K. O'Grady, and R. W. Chantrell, *J. Appl. Phys.* **76**, 6811 (1994).
- ⁸See, for example, C. Kuhrt, K. Schuitzlike, and L. Schultz, *J. Appl. Phys.* **73**, 6026 (1993); J. M. D. Coey, in these proceedings.